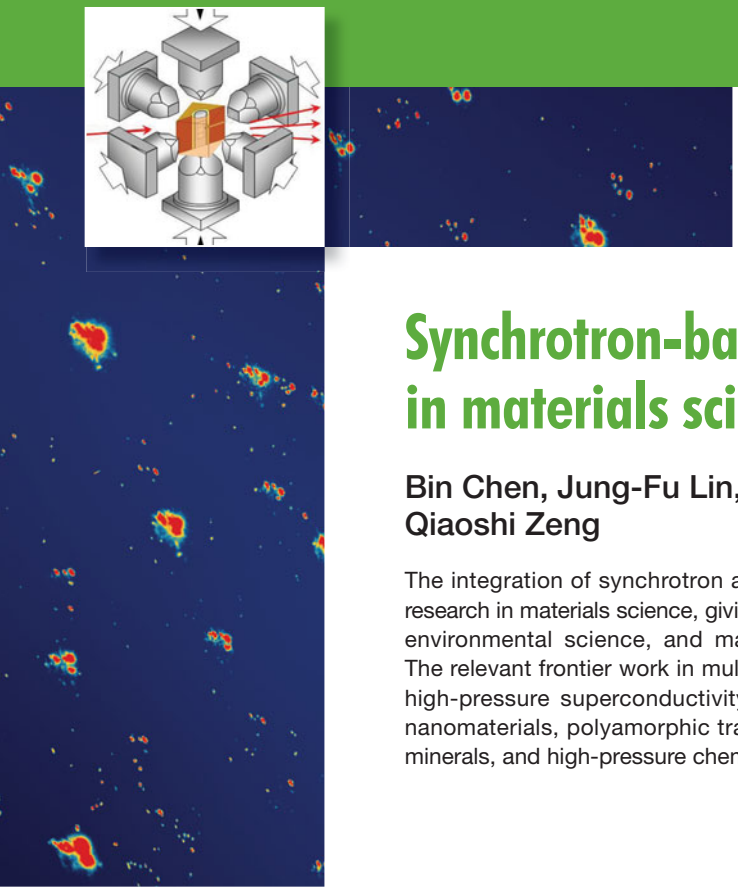

Synchrotron-based high-pressure research in materials science

Bin Chen, Jung-Fu Lin, Jiuhua Chen, Hengzhong Zhang, and Qiaoshi Zeng

The integration of synchrotron and high-pressure techniques has significantly advanced research in materials science, giving rise to many important discoveries in physics, chemistry, environmental science, and many other fields of physical and engineering sciences. The relevant frontier work in multiple disciplines is reviewed. The selected studies include high-pressure superconductivity, lattice dynamics of materials, plastic deformation of nanomaterials, polyamorphic transitions and devitrification in metallic glass, rheology of minerals, and high-pressure chemistry probing.

Introduction

The physical properties of materials are affected mainly by pressure, temperature, and composition. Pressures in nature span a wide range (**Figure 1**), from as low as 10^{-15} Pa in interstellar space, to as high as 10^{25} Pa at the center of white dwarf stars.[1] High-pressure science has been an important part of human knowledge since ancient times; however, it did not advance much until the advent of modern pressure devices. Vacuum techniques push the lower limits of attainable pressure, while on the upper end, diamond anvil cells (DACs), gas guns, and laser shock systems can generate pressures that are comparable to pressures at the center of a planet (Figure 1), enabling laboratory investigations of the physical properties of materials under various pressure conditions.

In recent decades, high-pressure research advanced rapidly with the development of pressure devices,[2,3] calibration, and various property-probing techniques.[4,5] The most popular and versatile pressure device is the DAC.[2,3]A sample is trapped between tiny flat faces (culet faces) of two opposing diamonds. A modest force applied across the wide "table" face of the diamond generates tremendous pressure on the sample through the "culet" face. The biggest advantage of a DAC is that diamond anvils are great optical probing windows, in addition to generating pressure. The disadvantage is that the sample size for DACs cannot be large (<20 μm), limiting investigations. In contrast, large-volume presses, a facility dedicated to determining the physical characteristics of materials under high pressure and temperature, allow for experiments on larger (millimeter-sized) samples with excellent temperature T and pressure P stability and uniformity, although the highest achievable pressures and temperatures in these devices (up to 40 GPa and 3000 K) are lower.[6]

A variety of dedicated synchrotron techniques (**Figure 2**) have promoted high-pressure research and have greatly impacted many disciplines, such as physics, chemistry, geophysics, and materials science.[5–10] Relevant discoveries include high-transition-temperature (T_c) superconductors,[11] the metallization of hydrogen,[12] the metal-to-insulator transition of alkali metals,[13,14] the polymorphisms of materials,[8,15] rheology of the Earth's mantle minerals,[16] deformation texturing of nanocrystals,[17,18] and long-range ordering in metallic glasses.[19] It is impossible to cover all frontier work in one article, as the impact of high-pressure research has extended to almost all physical sciences. Therefore, this article summarizes the advances in selected areas, but is mostly limited to static compression, mainly because it is a more laboratory-accessible approach.

Synchrotron-based high-pressure research in materials physics

Applied pressure has been shown to induce a number of intriguing physical phenomena, including phase transitions,

Bin Chen, Center for High Pressure Science & Technology Advanced Research, China; and Advanced Light Source, Lawrence Berkeley National Laboratory, USA; chenbin@hpstar.ac.cn and bchen@lbl.gov
Jung-Fu Lin, Center for High Pressure Science & Technology Advanced Research, China; and Department of Geological Sciences, The University of Texas at Austin, USA; linjf@hpstar.ac.cn
Jiuhua Chen, Mechanical and Materials Engineering Department, Florida International University, USA; and Center for High Pressure Science & Technology Advanced Research, China; chenjh@hpstar.ac.cn
Hengzhong Zhang, Center for High Pressure Science & Technology Advanced Research, China; hengzhong.zhang@hpstar.ac.cn
Qiaoshi Zeng, Center for High Pressure Science & Technology Advanced Research, China; zengqs@hpstar.ac.cn
doi:10.1557/mrs.2016.110

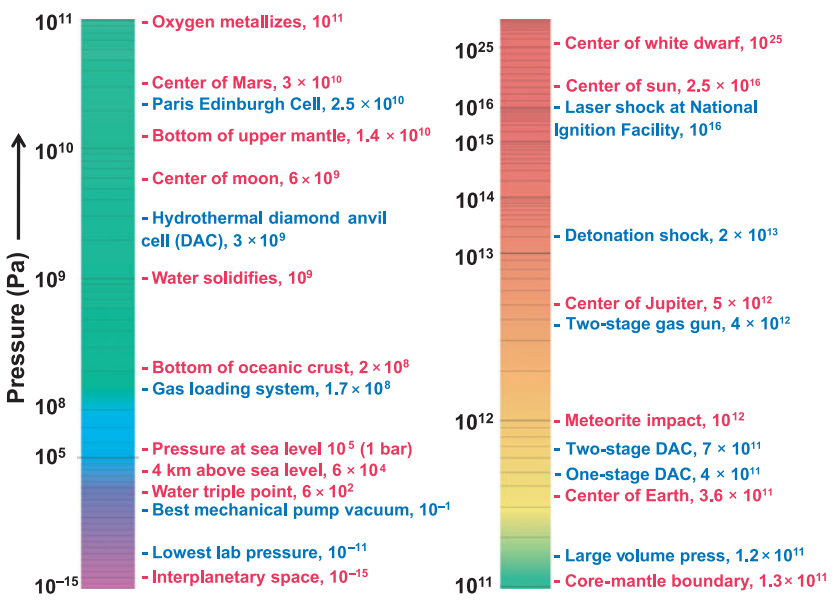

Figure 1. Pressure scale in the universe and pressure generation capabilities of lab devices.[1]

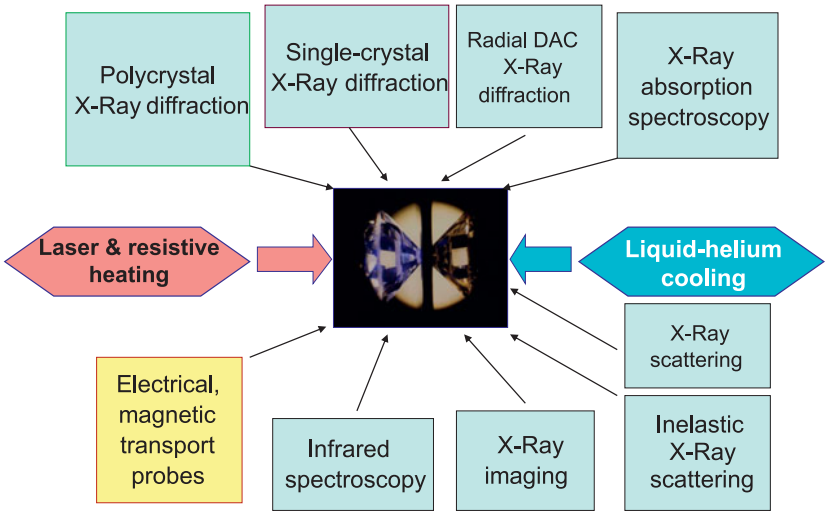

Figure 2. Integration of synchrotron techniques with pressurizing, heating, cooling, and electrical/magnetic transport probing techniques. Courtesy of Ho-Kwang Mao. Note: DAC, diamond anvil cell.

metallization and superconductivity,[20] syntheses of novel materials,[21] electronic and magnetic transitions, quantum critical points, and phonon softening.[6,22] The application of pressure increases the internal energy of the material and modifies interactions between neighboring atoms. We provide a few examples of high-pressure material physics research.

Pressure-induced superconductivity in pnictides

The recent discovery of iron-based superconductors (pnictides) has opened a new door to high-T_c superconductor studies.[23,24] Prominent features of these superconductors include: (1) superconductivity within an iron arsenide layer, in which Fe^{2+} exists in the parent antiferromagnetic (AFM) state; (2) formation of a spin-density wave (SDW) phase from the parent state; and (3) inducing superconductivity by suppressing the SDW state via chemical doping or applied external pressure. Applied pressure has been shown to effectively suppress AFM ordering and to induce a high critical temperature T_c in the pnictide system[25]—for example, superconductivity only occurs at high pressure in undoped "122" systems (**Figure 3**).

Synchrotron-based x-ray diffraction (XRD), Mössbauer spectroscopy, and nuclear resonant inelastic x-ray scattering spectroscopy (NRIXS) under high-pressure and low-temperature conditions are ideally suited to unravel the interplay among structure, magnetism, and phonon dynamics in pnictide systems.[26,27] High-pressure results have shown that magnetic and structural transitions are concurrently suppressed to much lower temperatures near a quantum critical pressure, where the AFM phase transforms into a bulk superconducting state (Figure 3). XRD and Mössbauer spectroscopy results have revealed that $SrFe_2As_2$ undergoes a magnetically ordered phase transition that is strongly coupled with the structural transition.[26] Magnetic ordering of $BaFe_2As_2$ surprisingly precedes the structural transition at high pressure in the parent compound (Figure 3), in sharp contrast to the chemical-doping case.[27] High-pressure low-temperature NRIXS techniques have been recently developed to reveal the role of phonon dynamics on the origin of superconductivity in pnictides.[28]

Lattice dynamics by inelastic x-ray scattering

Emerging at the forefront for exploring the lattice dynamics under high pressure are synchrotron-based inelastic x-ray scattering (IXS) techniques. IXS has been used to study acoustic and optical phonon dispersions and phonon density of states of materials at high pressure, unveiling very rich emergent phenomena, such as phonon anomalies,[29] acoustic phonon softening,[30] charge ordering, as well as mode hardening.[29,31] Specifically, IXS studies on the lattice dynamics of single-crystal molybdenum showed the phonon anomaly near the H-point of the Brillouin zone due to strong electron–phonon coupling, which decreases upon compression due to the Fermi level shift with respect to the relevant electronic bands.[32] High-pressure studies have also shown abnormal

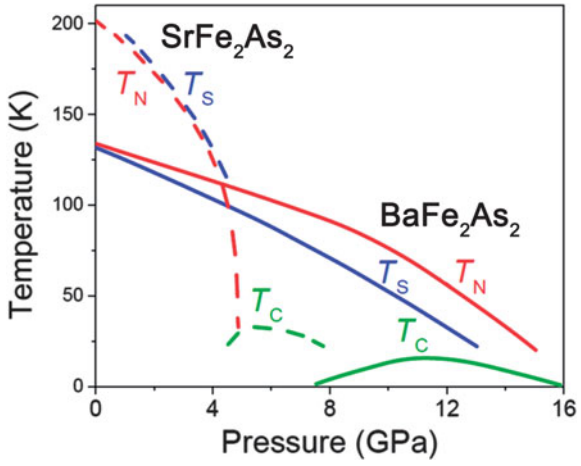

Figure 3. Magnetic and structural transition diagram of $BaFe_2As_2$ (solid lines) and $SrFe_2As_2$ (dashed lines) pnictides at high-pressure low-temperature. T_S: tetragonal-orthorhombic transition temperature based on x-ray diffraction results; T_N: paramagnetic-antiferromagnetic transition temperature based on Mössbauer results.[27,28] Note: T_c, superconducting critical temperature.

elastic and vibrational behaviors of single-crystal magnetite, which are attributed to the occurrence of octahedrally coordinated Fe^{2+}-Fe^{3+}-Fe^{2+} ions charge-ordering along [110] in the inverse spinel structure,[29] revealing a new phase diagram of magnetite at high-pressure low-temperature.[29] Recent advances in IXS techniques in a cryogenically cooled DAC and laser-heated DAC[33] provide new arsenals for studying fundamental materials physics under extreme conditions.

Plastic deformation of nanomaterials

Understanding the plastic deformation of nanocrystalline materials is a long-standing challenge. Various controversial observations, mainly on the existence of dislocations and the mechanisms for a reversed Hall–Petch effect, have been reported.[34–36] However, *in situ* observations of plastic deformation in ultrafine (sub-10 nm) nanocrystals has long been difficult, precluding the direct exploration of mechanics at the nanometer scale. Chen and co-workers plastically deformed nickel and spinel nanoparticles to pressures above 35 GPa[17] and observed texture development *in situ* during plastic deformation by using a radial diamond anvil cell (rDAC) XRD technique (incident x-rays are perpendicular to the compression axis) recently developed for geophysical research. The size of nanocrystals has long been viewed as limiting dislocation activity and associated deformation. Dislocation-mediated plastic deformation and texturing are expected to become inactive below a critical particle size, which is often thought to be between 10 and 30 nm, based on computer simulations[34] and transmission electron microscope analysis.[37] The new findings regarding the dislocation activities in ultrafine nickel[17] and $MgAl_2O_4$ demand considering the role of defects in the physical behaviors of nanomaterials.

Pressure-induced polyamorphic transition and devitrification in metallic glass

The polyamorphic transitions from a low-density amorphous state to a high-density amorphous state in glasses often result from increased atomic coordination. Such coordination increases and polyamorphism were thought to be impossible in nondirectional, densely packed metallic glass.[38] When combining *in situ* high-pressure XRD pair distribution function with molecular dynamics simulations, surprising polyamorphic transitions were obtained in $Ce_{55}Al_{45}$ metallic glass[39] and in $La_{32}Ce_{32}Al_{16}Ni_5Cu_{15}$ bulk metallic glass.[40] It was found that under high pressure, the 4*f* electrons of Ce in Ce-based metallic glass transform from the ambient localized state to an itinerant state, resulting in the polyamorphic transition. This new type of "electronic" polyamorphism in densely packed metallic glass is dictated by the Ce constituent and is fundamentally distinct from the polyamorphism that involves a coordination increase.[41,42] These studies have opened up a new research field on metallic glasses and have stimulated extensive studies on polyamorphic transitions in many other 4*f* elements-based metallic glass.

Whether a glass can have long-range structural order is a challenging question, because current experimental probes and theory are usually limited to local clusters in glasses. Using *in situ* high-pressure XRD, a $Ce_{75}Al_{25}$ metallic glass was found to crystallize into a single crystal of indefinite length at ~25 GPa in a DAC.[43] This discovery established direct linkage between single crystal and glass, two extreme end members in terms of structural order, providing a unique opportunity for observation of this otherwise invisible long-range order.[44]

Synchrotron-based high-pressure research in mineral physics—Probing mineral creep at mantle pressures

The rheological properties of minerals are indispensable for understanding the dynamics of the Earth's interior (consisting of, from surface to center, the upper mantle, transition zone, lower mantle, and core). In a traditional off-line deformation apparatus, creep experiments on minerals had never achieved pressure equivalents to depths greater than 100 km (3 GPa), as compared to the Earth's total depth of 6400 km (360 GPa, see Figure 1).[45] The application of synchrotron x-rays significantly extended the pressure range of creep experiments by directly modifying existing well-established high-pressure apparatuses.

The deformation-diamond synthesis apparatus (D-DIA) is a modification of the DIA apparatus (a cubic-type uniaxial compression press), developed for deformation experiments in conjunction with synchrotron beamlines to achieve a maximum pressure of 15 GPa (**Figure 4**a) at the Advanced Photon Source[46] and the National Synchrotron Light Source.[47] The maximum confining pressure (equivalent hydrostatic sample pressure) of D-DIA is limited to an achievable pressure of a regular DIA. The D-DIA apparatus has also been adopted at SPring8 (in Japan)[48] and the European Synchrotron Radiation

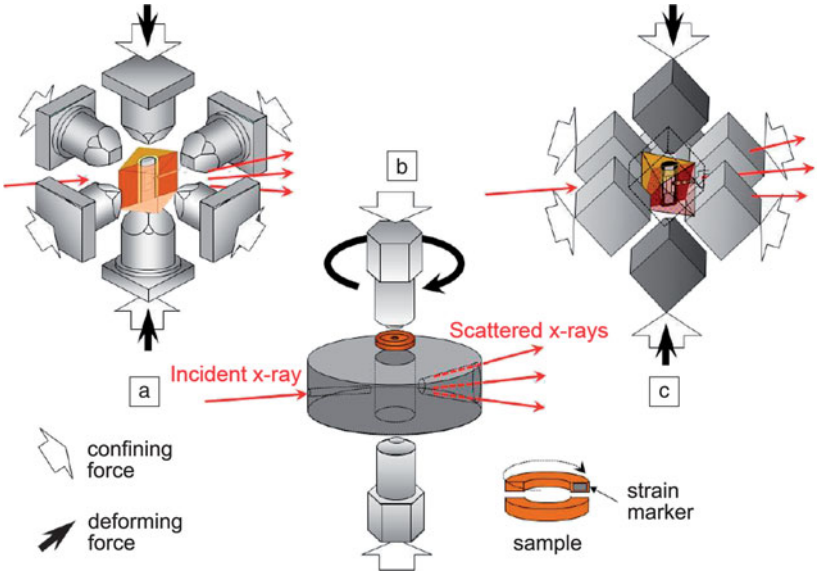

Figure 4. Sketch of principles of three synchrotron-based creep experiments. (a) Deformation-diamond synthesis (D-DIA): The confining pressure is achieved by advancing the six anvils in a DIA module simultaneously toward the cubic pressure medium with a cylindrical sample orientated vertically. Metallic foils are placed at each end of the sample as strain markers. Deforming forces, delivered by two differential rams, apply additional stress to the sample through the top and bottom anvils (black arrows) to induce creep at the confining pressure. (b) Rotational Drickamer apparatus: The confining pressure is achieved by advancing the opposed anvils toward a disc pressure medium with a ring-shape sample embedded inside. A metallic foil pressure marker is placed in the sample (orange) as shown. (c) Deformation-Tcup: The confining pressure is achieved by advancing the eight second-stage cubes in a Kawai-type module toward the octahedral pressure medium with a cylindrical sample orientated vertically. Metallic foils are placed at each end of the sample as strain markers. Deforming forces are delivered by two differential rams applying additional stress to the sample through the top and bottom cubes to induce creep at the confining pressure.

Facility (in Grenoble, France).[49] The pressure envelope of the D-DIA apparatus was recently advanced up to 20 GPa at SPring8.[48] In addition to creep experiments under constant strain rate, dynamic cyclical loading can also be applied in the D-DIA apparatus to explore the effects of temperature, pressure, frequency, and grain size on the energy dissipation of materials.[50] In the past decade, the D-DIA apparatuses at different synchrotron facilities have produced large amounts of data that have significantly advanced our knowledge on rheological properties of minerals (e.g., changes of dominant slip systems in olivine at deep upper mantle pressures).[48,51–55]

The rotational Drickamer apparatus (RDA) is a modification of the Drickamer apparatus (an opposed anvil press) with an added rotational actuator to deform samples through torsion[56] (Figure 4b), similar to high-pressure torsion for metal processing.[57] In the RDA, the opposed anvils are supported in confining rings, therefore, the achievable pressure is potentially higher than that in a D-DIA. In addition, the torsion experiment allows large strains (unlimited), which is particularly important for studying deformation-induced texture in a sample. A number of upper-mantle and transition-zone minerals have been investigated using RDA.[48,58–60] In a recent experiment, a bridgmanite (magnesium silicate perovskite) and magnesiowüstite (ferropericlase) aggregate sample was deformed in the RDA under the pressure and temperature conditions found in the top of the lower mantle. Researchers observed strain weakening in the sample,[16] which led to a hybrid model of mantle convection to explain the laboratory mineral physics results and geochemical and seismological observations.[61]

Another potential high-pressure deformation apparatus is a modified Tcup (a small version of a two-stage Kawai-type press). Since the Tcup is capable of reaching higher pressures than those attained with a DIA,[62] the deformation Tcup (D-Tcup) can potentially reach higher pressures as well. In the D-Tcup, the confining pressure is achieved with a Kawai-style module in which eight corner-truncated second-stage cubes advance toward the octahedral pressure medium (the center part in Figure 4c). Currently, the D-Tcup is not widely used in the mineral mechanics community, as it is still in an early stage of development. A test experiment with the D-Tcup has reached pressures up to approximately 19 GPa.[63]

Synchrotron-based high-pressure research in materials chemistry

Synchrotron in situ *study of materials synthesis at high pressures*

Using synchrotron XRD, the phase evolution of ZnO and GaN was monitored in reactions at pressures <9.2 GPa and temperatures up to 1500 K.[64] A solid solution of $(Ga_{1-x}Zn_x)(N_{1-x}O_x)$ in the wurtzite structure was produced at high pressure and temperature; this material has the potential of splitting water via visible light photocatalytic reactions.

As potentially cheaper alternatives to diamonds for cutting and shaping hard metals and ceramics, superhard noble metal nitrides and carbides were synthesized in DACs at high pressure and temperature, and the compressibility measured accordingly.[65–67] PtN was produced at above 45–50 GPa and 2000 K, and the bulk modulus was measured to be 372 GPa.[65] IrN_2 and OsN_2 were produced above 50 GPa and 2000 K, and the bulk modulus of $IrN_2$was measured to be 428 GPa.[67] PtC was produced at 70 GPa and 2600 K, and in this case, the bulk modulus was measured to be 301 GPa.[66]

Fullerene materials at high pressure and temperature

Fullerenes provide promising applications in medicine, solar cells, hydrogen storage, sensors, and strengthening of metals due to the specific buckyball structure and spectacular physical, chemical, and mechanical properties. Time-resolved synchrotron XRD showed that amorphization of C_{60} starts

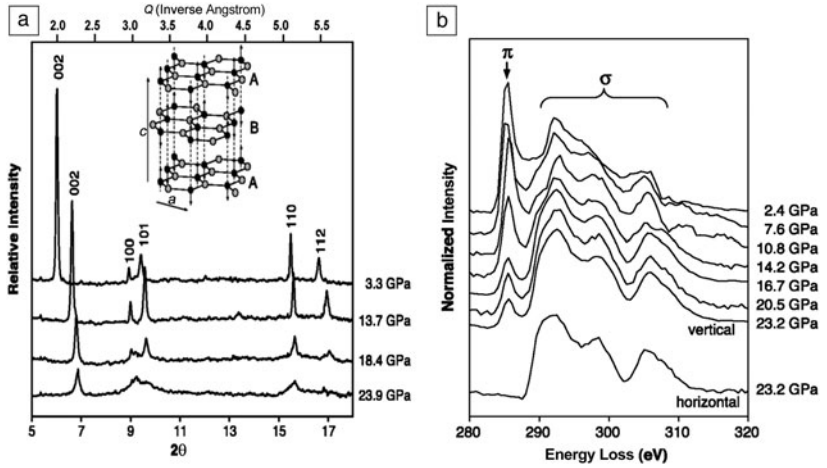

Figure 5. Change in chemical bonding in graphite under compression. (a) X-ray diffraction peaks broaden due to distortion of graphite basal planes under pressure. (b) Inelastic x-ray scattering (IXS) spectra showing one-half of the interplane carbon π bonds changed to σ bonds. Adapted with permission from Reference 7.© AAAS 2003. Note: *a*, lattice parameter; *c*, lattice parameter; θ, scattering angle; A, stacking layer; B, stacking layer; black sphere, layer-bridging carbon; gray sphere, nonbridging carbon; horizontal, IXS taken in the horizontal direction to probe carbon bonding in the *a*-plane; vertical, IXS taken in the vertical direction to probe carbon bonding in the *c*-plane.

at 700–900 K at 12.5 GPa and at 700–800 K at 14.3 GPa, due to breaking of the five-membered rings of the C_{60} molecules and collapsing of the original cage structure. The high-pressure behaviors of single-walled carbon nanotubes, polymerized fullerenes, and C_{60} peapods have also been investigated at room temperature[68] or upon heating.[69]

The chemical nature of carbon materials under pressure arises from the interchange between the σ and π C–C bonds that are primarily oriented on or normal to a graphite layer, respectively, at ambient pressure. Synchrotron x-ray inelastic scattering revealed that at a pressure of ~17 GPa, one-half of the π bonds between graphite layers convert to σ bonds between graphite layers, whereas the other half remain as π bonds in the high-pressure form (see **Figure 5**).[7] This change in bonding accounts for the observed formation of a new superhard phase of graphite.

Summary

Synchrotron x-ray analysis has become an increasingly important tool for high-pressure materials science. With new techniques, the structural, mechanical, electronic, optical, and many other physical and chemical properties of minute samples under ultrahigh pressures can be probed at atomic, nano-, micro-, and macroscales, making many previously impossible studies possible. Particularly noteworthy are investigations on pressure-induced superconductivity, structural and electronic properties of single and multilayered materials, and long-range structural ordering in metallic glasses.

The rheological properties of Earth and planetary materials can now be well characterized with controlled strain rates at high pressures using synchrotron XRD and imaging. The deformation mechanisms of nanomaterials can be examined *in situ* under compression. Synchrotron-based experimentation is anticipated to continuously impact a broad range of high-pressure studies of materials, allowing for more challenging explorations in multiple disciplines. For instance, an exciting outlook is that various probing techniques such as Brillouin/Raman/infrared/x-ray spectroscopy, XRD/scattering/imaging, and many others can be set up on the same beamline, allowing for a wide spectrum of investigations on the same area on a material sample and under the same conditions. More accurate and realistic information from such systematic examinations will provide more reliable understanding of the science of materials.

Acknowledgments

The authors acknowledge the support of NSAF Grant No. U1530402. B.C. thanks BL12.2.2, BL12.3.2, and BL1.4.3 of Advanced Light Source (ALS), Lawrence Berkeley National Lab, for the HPSTAR-ALS collaboration. The ALS is supported by the Director, Office of Science, Office of Basic Energy Sciences, of the US Department of Energy under Contract No. DE-AC02–05CH11231.

References

1. https://en.wikipedia.org/wiki/Orders_of_magnitude_(pressure).
2. P.F. McMillan, *Nat. Mater.* **4**, 715 (2005).
3. L. Dubrovinsky, N. Dubrovinskaia, E. Bykova, M. Bykov, V. Prakapenka, C. Prescher, K. Glazyrin, H.-P. Liermann, M. Hanfland, M. Ekholm, *Nature* **525**, 226 (2015).
4. H. Mao, P. Bell, J.T. Shaner, D. Steinberg, *J. Appl. Phys.* **49**, 3276 (1978).
5. M. Eremets, *High Pressure Experimental Methods* (Oxford University Press, New York, 1996).
6. Y.B. Wang, M. Rivers, S. Sutton, N. Nishiyama, T. Uchida, T. Sanehira, *Phys. Earth Planet. Inter.* **174**, 270 (2009).
7. W.L. Mao, H.-K. Mao, P.J. Eng, T.P. Trainor, M. Newville, C.-C. Kao, D.L. Heinz, J. Shu, Y. Meng, R.J. Hemley, *Science* **302**, 425 (2003).
8. Y. Iwasa, T. Arima, R. Fleming, T. Siegrist, O. Zhou, R. Haddon, L. Rothberg, K. Lyons, H. Carter, A. Hebard, *Science* **264**, 1570 (1994).
9. H. Jiang, R. Xu, C.-C. Chen, W. Yang, J. Fan, X. Tao, C. Song, Y. Kohmura, T. Xiao, Y. Wang, *Phys. Rev. Lett.* **110**, 205501 (2013).
10. X. Xi, X.-G. He, F. Guan, Z. Liu, R. Zhong, J. Schneeloch, T. Liu, G. Gu, X. Du, Z. Chen, *Phys. Rev. Lett.* **113**, 096401 (2014).
11. A. Drozdov, M. Eremets, I. Troyan, V. Ksenofontov, S. Shylin, *Nature* **525**, 73 (2015).
12. P. Loubeyre, F. Occelli, R. LeToullec, *Nature* **416**, 613 (2002).
13. Y. Ma, M. Eremets, A.R. Oganov, Y. Xie, I. Trojan, S. Medvedev, A.O. Lyakhov, M. Valle, V. Prakapenka, *Nature* **458**, 182 (2009).
14. T. Matsuoka, K. Shimizu, *Nature* **458**, 186 (2009).
15. L. Zhang, Y. Meng, W. Yang, L. Wang, W.L. Mao, Q.-S. Zeng, J.S. Jeong, A.J. Wagner, K.A. Mkhoyan, W. Liu, *Science* **344**, 877 (2014).
16. J. Girard, G. Amulele, R. Farla, A. Mohiuddin, S.-I. Karato, *Science* **351**, 144 (2016).
17. B. Chen, K. Lutker, S.V. Raju, J. Yan, W. Kanitpanyacharoen, J. Lei, S. Yang, H.-R. Wenk, H.-K. Mao, Q. Williams, *Science* **338**, 1448 (2012).
18. B. Chen, K. Lutker, J. Lei, J. Yan, S. Yang, H.-K. Mao, *Proc. Natl. Acad. Sci. U.S.A.* **111**, 3350 (2014).
19. D.Z. Chen, C.Y. Shi, Q. An, Q. Zeng, W.L. Mao, W.A. Goddard, J.R. Greer, *Science* **349**, 1306 (2015).

20. D.Y. Kim, R.H. Scheicher, H.-K. Mao, T.W. Kang, R. Ahuja, *Proc. Natl. Acad. Sci. U.S.A.* **107**, 2793 (2010).
21. W. Zhang, A.R. Oganov, A.F. Goncharov, Q. Zhu, S.E. Boulfelfel, A.O. Lyakhov, E. Stavrou, M. Somayazulu, V.B. Prakapenka, Z. Konôpková, *Science* **342**, 1502 (2013).
22. H.-K. Mao, C. Kao, R.J. Hemley, *J. Phys. Condens. Matter* **13**, 7847 (2001).
23. Y. Kamihara, H. Hiramatsu, M. Hirano, R. Kawamura, H. Yanagi, T. Kamiya, H. Hosono, *J. Am. Chem. Soc.* **128**, 10012 (2006).
24. Y. Kamihara, T. Watanabe, M. Hirano, H. Hosono, *J. Am. Chem. Soc.* **130**, 3296 (2008).
25. C.W. Chu, B. Lorenz, *Physica C* **469**, 385 (2009).
26. J.J. Wu, J.F. Lin, X.C. Wang, Q.Q. Liu, J.L. Zhu, Y.M. Xiao, P. Chow, C.Q. Jin, *Sci. Rep.* **4**, 3685 (2014).
27. J.J. Wu, J.-F. Lin, X.C. Wang, Q.Q. Liu, J.L. Zhu, Y.M. Xiao, P. Chow, C. Jin, *Proc. Natl. Acad. Sci. U.S.A.* **110**, 17263 (2013).
28. W. Bi, J. Zhao, J.-F. Lin, Q. Jia, M.Y. Hu, C. Jin, R. Ferry, W. Yang, V. Struzhkin, E.E. Alp, *J. Synchrotron Radiat.* **22**, 760 (2015).
29. J.-F. Lin, J. Wu, J. Zhu, Z. Mao, A.H. Said, B.M. Leu, J. Cheng, Y. Uwatoko, C. Jin, J. Zhou, *Sci. Rep.* **4**, 6282 (2014).
30. J.-F. Lin, S.T. John, E.E. Alp, J. Zhao, M. Lerche, W. Sturhahn, Y. Xiao, P. Chow, *Phys. Rev. B Condens. Matter* **84**, 064424 (2011).
31. I. Jarrige, J.-P. Rueff, S. Shieh, M. Taguchi, Y. Ohishi, T. Matsumura, C.-P. Wang, H. Ishii, N. Hiraoka, Y. Cai, *Phys. Rev. Lett.* **101**, 127401 (2008).
32. D.L. Farber, M. Krisch, D. Antonangeli, A. Beraud, J. Badro, F. Occelli, D. Orlikowski, *Phys. Rev. Lett.* **96**, 115502 (2006).
33. J.-F. Lin, W. Sturhahn, J. Zhao, G. Shen, H.-K. Mao, R.J. Hemley, *Science* **308**, 1892 (2005).
34. J. Schiøtz, F.D. Di Tolla, K.W. Jacobsen, *Nature* **391**, 561 (1998).
35. M. Chen, E. Ma, K.J. Hemker, H. Sheng, Y. Wang, X. Cheng, *Science* **300**, 1275 (2003).
36. L. Lu, X. Chen, X. Huang, K. Lu, *Science* **323**, 607 (2009).
37. Z. Shan, E. Stach, J. Wiezorek, J. Knapp, D. Follstaedt, S. Mao, *Science* **305**, 654 (2004).
38. H.W. Sheng, W.K. Luo, F.M. Alamgir, J.M. Bai, E. Ma, *Nature* **439**, 419 (2006).
39. H. Sheng, H. Liu, Y. Cheng, J. Wen, P. Lee, W. Luo, S. Shastri, E. Ma, *Nat. Mater.* **6**, 192 (2007).
40. Q. Zeng, Y. Li, C. Feng, P. Liermann, M. Somayazulu, G. Shen, H.-K. Mao, R. Yang, J. Liu, T. Hu, *Proc. Natl. Acad. Sci. U.S.A.* **104**, 13565 (2007).
41. M. Guthrie, C. Tulk, C. Benmore, J. Xu, J. Yarger, D. Klug, J. Tse, H. Mao, R. Hemley, *Phys. Rev. Lett.* **93**, 115502 (2004).
42. C. Meade, R.J. Hemley, H. Mao, *Phys. Rev. Lett.* **69**, 1387 (1992).
43. Q.S. Zeng, Y. Ding, W.L. Mao, W. Luo, A. Blomqvist, R. Ahuja, W. Yang, J. Shu, S.V. Sinogeikin, Y. Meng, D.L. Brewe, J.Z. Jiang, H.K. Mao, *Proc. Natl. Acad. Sci. U.S. A.* **106**, 2515 (2009).
44. Q.S. Zeng, H.W. Sheng, Y. Ding, L. Wang, W.G. Yang, J.Z. Jiang, W.L. Mao, H.K. Mao, *Science* **332**, 1404 (2011).
45. S.-I. Karato, D.J. Weidner, *Elements* **4**, 191 (2008).
46. Y.B. Wang, W.B. Durham, I.C. Getting, D.J. Weidner, *Rev. Sci. Instrum.* **74**, 3002 (2003).
47. J.H. Chen, L. Li, D. Weidner, M. Vaughan, *Phys. Earth Planet. Inter.* **143–144**, 347 (2004).
48. T. Kawazoe, N. Nishiyama, Y. Nishihara, T. Irifune, *Phys. Earth Planet. Inter.* **183**, 190 (2010).
49. J. Guignard, W.A. Crichton, *Rev. Sci. Instrum.* **86**, 085112 (2015).
50. L. Li, D.J. Weidner, *Rev. Sci. Instrum.* **78**, 053902 (2007).
51. E. Amiguet, P. Raterron, P. Cordier, H. Couvy, J.C. Chen, *Phys. Earth Planet. Inter.* **177**, 122 (2009).
52. J. Girard, J.H. Chen, P. Raterron, C.W. Holyoke, *Phys. Earth Planet. Inter.* **216**, 12 (2013).
53. L. Li, P. Raterron, D. Weidner, J.H. Chen, *Phys. Earth Planet. Inter.* **138**, 113 (2003).
54. P. Raterron, J. Chen, L. Li, D. Weidner, P. Cordier, *Am. Mineral.* **92**, 1436 (2007).
55. P. Raterron, J.H. Chen, T. Geenen, J. Girard, *Phys. Earth Planet. Inter.* **188**, 26 (2011).
56. D. Yamazaki, S. Karato, *Rev. Sci. Instrum.* **72**, 4207 (2001).
57. A. Zhilyaev, T. Langdon, *Prog. Mater. Sci.* **53**, 893 (2008).
58. R. Farla, G. Amulele, J. Girard, N. Miyajima, S. Karato, *Phys. Chem. Miner.* **42**, 541 (2015).
59. Y. Nishihara, D. Tinker, T. Kawazoe, Y.S. Xu, Z.C. Jing, K.N. Matsukage, S.I. Karato, *Phys. Earth Planet. Inter.* **170**, 156 (2008).
60. N. Nishiyama, Y.B. Wang, T. Irifune, T. Sanehira, M.L. Rivers, S.R. Sutton, D. Cookson, *J. Synchrotron Radiat.* **16**, 742 (2009).
61. J. Chen, *Science* **351**, 122 (2016).
62. M. Vaughan, D. Weidner, Y. Wang, J. Chen, C.C. Koleda, I.C. Getting, *Rev. High Press. Sci. Technol.* **7**, 1520 (1998).
63. S.A. Hunt, D.J. Weidner, R.J. McCormack, M.L. Whitaker, E. Bailey, L. Li, M.T. Vaughan, D.P. Dobson, *Rev. Sci. Instrum.* **85**, 085103 (2014).
64. H. Chen, L. Wang, J. Bai, J.C. Hanson, J.B. Warren, J.T. Muckerman, E. Fujita, J.A. Rodriguez, *J. Phys. Chem. C* **114**, 1809 (2010).
65. E. Gregoryanz, C. Sanloup, M. Somayazulu, J. Badro, G. Fiquet, H.-K. Mao, R.J. Hemley, *Nat. Mater.* **3**, 294 (2004).
66. S. Ono, T. Kikegawa, Y. Ohishi, *Solid State Commun.* **133**, 55 (2005).
67. A.F. Young, C. Sanloup, E. Gregoryanz, S. Scandolo, R.J. Hemley, H.-K. Mao, *Phys. Rev. Lett.* **96**, 155501 (2006).
68. S. Kawasaki, Y. Matsuoka, A. Yao, F. Okino, H. Touhara, K. Suito, *J. Phys. Chem. Solids* **65**, 327 (2004).
69. S. Kawasaki, Y. Matsuoka, T. Yokomae, Y. Nojima, F. Okino, H. Touhara, H. Kataura, *Carbon* **43**, 37 (2005). □